STRESS CORROSION CRACKING OF NICKEL BASE SUPERALLOYS IN AERATED SUPERCRITICAL WATER

L. Fournier, David Delafosse, C Bosch, Thierry Magnin

Fournier, L., Delafosse, D., Bosch, C., & Magnin, T. (2001). Stress Corrosion Cracking of Nickel Base Superalloys in Aerated Supercritical Water. In Proceedings of the 2001 NACE Corrosion Conference. Houston, Texas: NACE. . Paper 01361
http://www.nace.org/cstm/Store/Product.aspx?id=066dfc18-f20d-48e9-84c7-4d440960183c

STRESS CORROSION CRACKING OF NICKEL BASE SUPERALLOYS IN AERATED SUPERCRITICAL WATER

L. Fournier[†], D. Delafosse, C. Bosch and T. Magnin
Ecole des Mines de St-Etienne, Centre SMS, URA CNRS 1884
158 Cours Fauriel, 42023 Saint-Etienne Cedex 02, France

ABSTRACT

The stress corrosion cracking behaviour of two nickel base superalloys (A718 and A690) is investigated in aerated supercritical water by means of constant extension rate tensile (CERT) tests at 400°C and 25 MPa. Alloy 718 is observed to be extremely sensitive to intergranular stress corrosion cracking (IGSCC) while alloy 690 is found to be immune to IGSCC. CERT tests are also carried out in air and under vacuum on both alloys at 600°C, i.e. in a temperature domain where nickel base superalloys exhibit oxygen embrittlement. The results obtained strongly suggest that oxidation is controlling both the stress corrosion crack initiation and propagation stages of nickel base superalloys in aerated supercritical water. In the light of these results, the main issue of material selection for the construction of supercritical water oxidation (SCWO) reactors is discussed.

Keywords: stress corrosion cracking, nickel base superalloy, supercritical water oxidation (SCWO), alloy 718, alloy 690, oxygen embrittlement.

[†] is currently a research fellow at the University of Michigan, Nuclear Engineering and Radiological Sciences Department, USA.

INTRODUCTION

In the SCWO process, organic wastes are oxidised into carbon dioxide and water by the molecular oxygen added to water in the supercritical state (T>374°C and P>22 MPa). Due to its low values of density and dielectric constant, supercritical water acts as a non-polar solvent in

which organic compounds and oxygen exhibit a total miscibility. Therefore, conversion rates typically greater than 99.99 % are obtained, making SCWO a very effective and promising technology.
However, the reactor is subjected to a highly aggressive environment and material selection, through corrosion resistance, is a major problem in the context of development of SCWO. Nickel base superalloys, such as alloy 625 and alloy 718, have been selected for the construction of the first pilot reactors. Under SCWO conditions, these materials have been shown to exhibit significant general corrosion rates ranging from 2 mm/year to 12 mm/year (1-2). Furthermore, stress corrosion cracking (SCC) has also been observed (3) and is believed to be a key issue.
In this context, the aim of this work was to investigate, for the first time, the SCC behaviour of nickel base superalloys in aerated supercritical water. A test autoclave was designed and CERT tests were performed at 400°C and 25 MPa on smooth specimens of two different alloys: A718 and A690. Alloy 718 is a nickel base superalloy (18 wt% chromium) mainly strengthened by γ'' precipitates and widely used for highly stressed components in high temperature applications as well as in pressurised water reactor (PWR) systems. Alloy 690 (29 wt% chromium) is a solution hardened nickel base superalloy.
Additionally, our objective was to gain insights in the mechanisms that may be responsible for SCC of nickel base superalloys in supercritical water. Kriksunov and Macdonald (4) have emphasized that the transition from subcritical to supercritical water was accompanied by a transition from the corrosion mechanisms characteristic of a liquid phase to those of a gas phase, i.e. from an ionic mechanism to a molecular mechanism. Nickel base superalloys being sensitive to oxygen embrittlement in the temperature range 500°C to 700°C (5-10), the possible role played by oxygen in the SCC process of nickel base superalloys in aerated supercritical water was examined here. For this purpose, CERT tests were performed in air and under vacuum at 600°C on both A718 and A690. Results were compared with the CERT tests carried out in aerated supercritical water.

EXPERIMENTAL PROCEDURE

The chemical compositions of the investigated alloys are given in Table 1. Alloy 718 was conventionally heat treated as follows: 955°C for 1 hour then furnace cooled; 720°C for 8 hours then cooled at a rate of 50°C per hour; 620°C for 8 hours and then air cooled. The average grain size was about 20 µm. Blocky primary niobium carbide precipitates were observed, mostly at grain boundaries (Figure 1.a) which is consistent with the findings of other authors (11-12). TEM examination showed γ'' (Ni_3Nb) precipitates with a mean diameter between 30 nm and 50 nm. Alloy 690 was studied in the solution annealed conditions with a grain size of about 60 µm. TEM examination revealed discrete precipitation of $M_{23}C_6$ carbides at grain boundaries.
CERT tests in supercritical water were performed in a test autoclave attached to a SCHENCK RMC100 mechanical test machine. A schematic of the test autoclave is given in Figure 2.a. It consists of a tubular pressure vessel [1] and two smooth cylindrical axes [2 and 3]. The tensile specimen [4] is attached to one of the ends of each of these axes by means of a threaded nut [5] which hold two alumina clevices. The other ends of the axes are fixed to the frame (axis 2) or to the cross-head (axis 3) of the testing machine. The pressurised volume around the test specimen is about 40 cm^3 and the pressure confinement is handled by both a nitrile mobile seal that is water cooled and a metal-metal gasket. A height cartridge heaters system, a type K thermocouple, and a PID regulator were used to monitor and control the temperature of the fluid. Smooth tensile specimens with 10 mm gage length and 5 mm diameter (Figure 2.b) were polished to a 3 µm finish before testing.
CERT tests in air and under vacuum (2×10^{-5} mbar) were conducted on a different system already described elsewhere (13). For these tests, smooth tensile specimens with 15 mm gage length and 4 mm diameter (Figure 2.c) also polished to a 3 µm finish were used.

RESULTS

Stress corrosion cracking

Alloy 718. Figure 3 displays the stress-strain curves of alloy 718 specimens strained at 10^{-6} s^{-1} and 400°C in air and in supercritical water at 25 MPa. In supercitical water, the ductility of alloy 718 is significantly decreased in comparison to air. Interestingly, the final fracture in supercritical water does not occur in an abrupt way but by a continuous decrease of the flow stress down to zero. It may also be noted that the specimen strained in air exhibits serrated flow, i.e. Portevin – Le Chatelier effect. The serrations occur after a finite amount of plastic strain close to 5% and persist up to fracture. Following the nomenclature proposed by Chihab et al. (14), the plastic instabilities observed can be designated as type C. In contrast, as its fracture strain is below the critical strain for the occurrence of plastic instabilities, the specimen deformed in supercritical water exhibits a continuous plastic flow.

As shown in Figure 4, the specimen strained in supercritical water fails in a brittle manner, with almost no reduction in area. The whole fracture surface of the specimen is intergranular. The absence of ductile tearing may explain the final fracture by the continuous decrease of the flow stress down to zero mentioned earlier. Several secondary cracks can also be noticed on the fracture surface.

The examination of the surface of the specimen strained in supercritical water shows that crack initiation occurs at the vicinity of oxidized particles (Figure 5.a). These particles were identified as niobium carbides by EDX analysis (Figure 5.b), which suggests that oxidation and swelling of the primary niobium carbides is responsible for crack initiation in supercritical water.

In contrast, at 400°C in air, for the same strain rate of 10^{-6} s^{-1}, fracture occurs in a ductile way by shearing on a macroscopic plane 45° to the tensile axis (Figure 6). This particular mode of failure has already been observed for alloy 718, and was found to coincide with the manifestation of type C plastic instabilities (7).

Alloy 690. The stress-strain curves of alloy 690 specimens strained at 10^{-6} s^{-1} and 400°C, in air and in supercritical water at 25 MPa, are plotted in Figure 7. Clearly, the environment has no significant effect on the fracture strain. Additionally, alloy 690 strained in supercritical water fails in a ductile way with an important reduction in area (Figure 8). In contrast to alloy 718, in the same experimental conditions, alloy 690 seems to be immune to SCC.

Oxygen embrittlement

Alloy 718. Figure 9 displays the stress-strain curves of alloy 718 specimens strained at 5×10^{-7} s^{-1} in air and under vacuum at 600°C. The oxidising environment leads to a significant decrease in the ductility of alloy 718, in comparison to the inert environment. The specimen strained under vacuum exhibits a ductile mode of failure, while the specimen strained in air fails in an intergranular way (Figure 10). The SEM examination of the surface of the specimen strained in air shows that crack initiation occurs, like in aerated supercritical water, at the vicinity of oxidised primary niobium carbides (Figure 11).

Alloy 690. Alloy 690 specimens strained at 5×10^{-7} s^{-1} in air and under vacuum at 600°C exhibit similar fracture strain (Figure 12) and a ductile mode of failure (Figure 13).

DISCUSSION

Stress corrosion cracking mechanism

It is well established that SCC results from local corrosion – deformation interactions at the crack tip (15). In aqueous solution, the hydrogen produced by the cathodic reaction of the corrosion process (ionic mechanism) inside a crack is believed to contribute to its propagation for various material – environment systems, such as austenitic stainless steel in boiling $MgCl_2$ (16) and nickel base alloys in

the primary water of PWR (17). However, in supercritical water, as emphasized by Kriksunov and Macdonald (4), the corrosion process is controlled by a molecular mechanism rather than by an ionic mechanism. As a consequence, the study of the SCC process of nickel base superalloys in supercritical water requires the investigation of possible molecular mechanisms.

In the present study, we examined the role that oxygen embrittlement may play in the SCC process of nickel base superalloys in aerated supercritical water. Interestingly, A718 and A690 were found to exhibit similar behaviour when strained in aerated supercritical water (400°C and 25 MPa) and in air at 600°C. For alloy 718, in both environments, crack initiation resulted from oxidation and swelling of primary niobium carbides and crack propagation was purely intergranular. Conversely, alloy 690 was found to be immune to any environmental effect in both environments.

Oxygen embrittlement of nickel and its alloys has been first documented by Bricknell and Woodford (5). They observed that specimens exposed to air at a temperature typically greater than 1000°C exhibit an important loss of ductility, coupled with intergranular fracture when straining is performed at lower temperature. In the temperature range 500°C to 650°C, nickel base superalloys have also been shown to be sensitive to oxygen embrittlement under tensile dynamic loading. Pandey et al. (6) have reported an important loss of ductility in alloy X-750 strained in air at 625°C, in comparison to vacuum. Several authors (8-10) have also observed that crack growth rates in air were several orders of magnitude higher than under vacuum, and that fracture mode changed from transgranular under vacuum to intergranular in air, during low cycle fatigue tests performed on compact tension specimens of alloy 718 at 650°C. Finally, recent CERT tests carried out in air and under vacuum at 5×10^{-7} s^{-1} showed that alloy 718 was embrittled by oxygen at 500°C (7), i.e. at a temperature relevant to the SCWO process.

From a mechanistic point of view, Bricknell and Woodford (5) clearly demonstrated that grain boundary penetration by oxygen is responsible for oxygen embrittlement above 1000°C. At lower temperature, Molins et al. (8) proposed a different mechanism to explain alloy 718 oxygen embrittlement. These authors have investigated the influence of oxygen partial pressure on both crack growth rate of compact tension specimens during creep-fatigue tests at 650°C, and composition of the oxide formed during the early stages of the oxidation process. They observed the existence of a slow crack growth rate regime at an oxygen partial pressure below 10^{-3} mbar and a three orders of magnitude higher crack growth rate regime beyond 10^{-3} mbar. The increase in crack growth rate was found to coincide with a transition in the cracking path from transgranular to intergranular. They also observed that at oxygen partial pressures in excess of 10^{-3} mbar, the formation of a nickel-rich oxide was favoured in the early stages of the oxidation process, while at oxygen partial pressure below 10^{-3} mbar, the formation of a chromium-rich oxide was favoured. On the basis of the observation by Hancock (18) that metal oxidation by cationic diffusion through the oxide results in vacancy generation, Molins et al. (8) suggested that nickel oxide formation at the crack tip and the resulting vacancy injection were responsible for the intergranular embrittlement by oxygen.

The application of these mechanisms to explain SCC in supercritical water is certainly not straightforward. However, both mechanisms may be considered. Internal oxidation has been recently proposed as a plausible mechanism to explain IGSCC of alloy 600 in the primary water of PWR (19) and several studies have been carried out to test its validity (20-21). Additional experiments aimed at determining the composition and the mechanism of growth (anionic or cationic) of the oxide films formed on nickel base superalloys in supercritical water would allow to establish whether vacancy injections can be invoked.

Application to material selection for the SCWO process

As shown in the result section, the presence of oxidation sensitive particles is highly detrimental to the resistance of nickel base superalloys to stress corrosion crack initiation in aerated supercritical water. This suggests that the choice of nickel base superalloy hardened by precipitates, which either contain TiC or NbC, is not suitable for the construction of SCWO reactors. In contrast, the good

resistance to SCC exhibited by alloy 690 during CERT test in aerated supercritical water suggests that solid solution hardened nickel base superalloy may be suitable as a construction material.
At this stage, use of fracture mechanics testing techniques would be particularly interesting in order to get information on the resistance to stress corrosion crack propagation of these nickel base superalloys in supercritical water. However, Speidel and Magdowski (22) have shown that an increase in yield strength significantly increases the stress corrosion crack growth rates in alloy 600 specimens with different degree of cold-work in de-aerated water at 350°C. Therefore, it is very likely that precipitation hardened nickel base superalloys would exhibit a much higher stress corrosion crack growth rate in supercritical water than solid solution hardened nickel base superalloys, which have a much lower yield strength.
Additionally, the chromium content of the nickel base superalloy may be of particular importance. Molins et al. (8) have performed crack propagation tests under various oxygen partial pressure on binary Ni-Cr alloys with 20 wt% and 30 wt% of chromium, respectively. Like for alloy 718, for the alloy with 20 wt% of chromium, they observed the existence of a transition partial pressure between a slow crack growth rate regime and a high crack growth rate regime at 10^{-3} mbar. Conversely, the alloy with 30 wt% of chromium only exhibited a slow crack growth rate regime suggesting that it was immune to oxygen embrittlement. Moreover, an important chromium content, through the formation of a protective oxide film, may guarantee a better resistance to general corrosion as well as a better resistance to crack initiation in supercritical water.

CONCLUSIONS

In aerated supercritical water (400 °C, 25 MPa), alloy 718 strained at 10^{-6} s^{-1} is sensitive to SCC. Crack initiation results from oxidation and swelling of primary niobium carbides and crack propagation is purely intergranular. In the same experimental conditions, alloy 690 is immune to SCC.
At 600°C, alloy 718 is also sensitive to oxygen embrittlement. CERT test performed at 5×10^{-7} s^{-1} showed that this environmental effect is accompanied by a significant decrease of the fracture strain in air compared to vacuum, and a change in the fracture mode from transgranular under vacuum to intergranular in air. Like in supercritical water, crack initiation results from oxidation and swelling of primary niobium carbides. Conversely, in the same experimental conditions, alloy 690 is not sensitive to oxygen embrittlement.
These similarities suggest that oxygen may play a key role in both the stress corrosion crack initiation and propagation mechanisms of nickel base superalloys in aerated supercritical water.

ACKNOWLEDGMENTS

The authors gratefully acknowledge Anjou Recherche, CNIM, CNRS and Ecodev for their financial support as well as Aubert et Duval for supplying the materials.

REFERENCES

1. R. M. Latanision, Corrosion Science, 51 (1995): p. 270.
2. P. Kritzer, N. Boukis, E. Dinjus, Materials and Corrosion, 49 (1998): p. 831.
3. R. M. Latanision, R. W. Shaw, ″Corrosion in supercritical water oxidation systems,″ Workshop Summary, The Energy Laboratory, MIT, 6-7 May, 1993.
4. L. B. Kriksunov, D. D. Macdonald, Journal of the Electrochemical Society, 142 (1995): p. 4069.
5. R. H. Bricknell, D. A. Woodford, Metallurgical Transactions, 12 (1981): p.425.
6. M. C. Pandey, D. M. R. Taplin, A. K. Mukherjee, Metallurgical Transactions, 15 (1984): p.1763.
7. L. Fournier, PhD thesis, Ecole Nationale Superieure des Mines de St-Etienne, France (2000).

8. R. Molins, G. Hochstetter, J. C. Chassaigne, E. Andrieu, Acta Materialia, 2 (1997): p. 663.
9. M. Clavel, A. Pineau, Materials Science and Engineering, 55 (1982): p.157.
10. A. Diboine, A. Pineau, Fatigue and Fracture of Engineering Material Structure, 10 (1987): p.141.
11. S. Fox, J. W. Brooks, M. H. Loretto, R. E. Smallman, ″Influence of carbides on the mechanical properties on inconel 718,″ Seventh International Conference on Strength of Metals and Alloys, (Pergamon Press, 1986).
12. M. Sundararaman, P. Mukhopadhyay, High Temperature Materials and Processes, 11 (1993): p.351.
13. A. Harabasz, K. Wolski, T. Magnin, M. Biscondi, Materials Science Forum, 294-296 (1999): p. 677.
14. K. Chihab, Y. Estrin, L.P. Kubin, J. Vergnol, Scripta Metal. 21 (1987): p 203.
15. T. Magnin, Advances in Corrosion-Deformation Interactions (Zurich: Trans Tech. Publications Ltd, 1996).
16. D. Delafosse, J. P. Chateau, A. Chambreuil, T. Magnin, Materials Science and Engineering, 234-236 (1997): p.889.
17. T. Magnin, F. Foct, O. de B, ″Hydrogen effects on PWR SCC mechanisms in monocrystalline and polycrystalline alloy 600,″ Ninth International Symposium on Environmental Degradation of Materials in Nuclear Power Systems – Water Reactors, (The Minerals, Metals and Materials Society, 1999).
18. P. Hancock, ″Influence of vacancies produced by oxidation on the mechanical properties of Ni and Ni-Cr alloys,″ Vacancies 1976, (Met. Soc., 1977).
19. P. M. Scott, M. Le Calvar, ″Some possible mechanisms of intergranular stress corrosion cracking of alloy 600 in PWR primary water,″ Sixth International Symposium on Environmental Degradation of Materials in Nuclear Power Systems – Water Reactors, (The Minerals, Metals and Materials Society, 1993).
20. L. E. Thomas, S. M. Bruemmer, ″Insights into environmental degradation mechanisms from analytical transmission electron microscopy of SCC cracks,″ Ninth International Symposium on Environmental Degradation of Materials in Nuclear Power Systems – Water Reactors, (The Minerals, Metals and Materials Society, 1999).
21. R. C. Newman, T. S. Gendron, P. M. Scott, ″Internal oxidation and embrittlement of alloy 600,″ Ninth International Symposium on Environmental Degradation of Materials in Nuclear Power Systems – Water Reactors, (The Minerals, Metals and Materials Society, 1999).
22. M. O. Speidel, R. Magdowski, ″Stress corrosion cracking of nickel base alloys in high temperature water,″ Sixth International Symposium on Environmental Degradation of Materials in Nuclear Power Systems – Water Reactors, (The Minerals, Metals and Materials Society, 1993).

TABLE 1 – Chemical composition (in weight %) of the alloy used in this study.

	Ni	Cr	Fe	Nb	Mo	Al	Ti	Cu	Mn	Si	Co	C	S	B	P
A718	53.67	17.95	bal.	5.27	2.98	0.52	0.92	0.1	0.04	0.07	0.04	0.033	0.006	0.005	0.002
A690	bal.	28.64	10.23	-	-	1.27	0.26	-	0.3	0.256	-	0.023	<0.005	-	<0.020

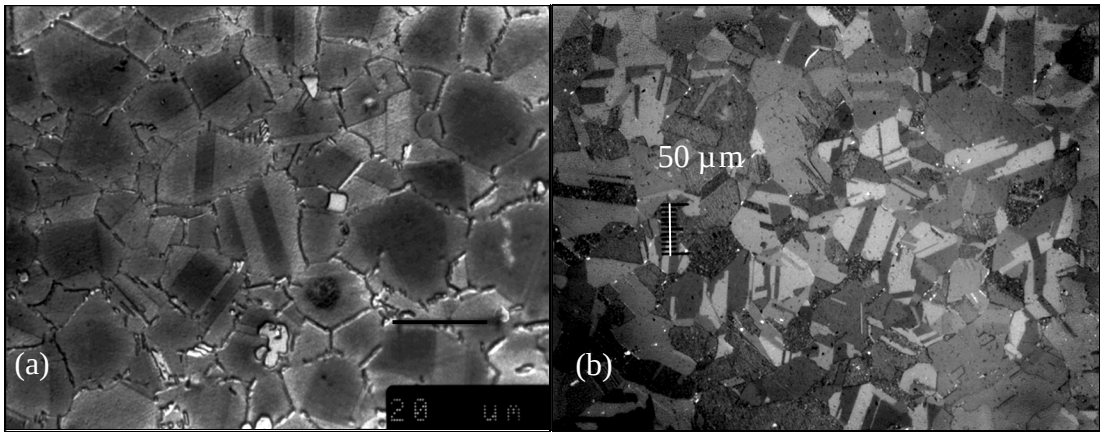

FIGURE 1 – Microstructure of (a) alloy 718 and (b) alloy 690.

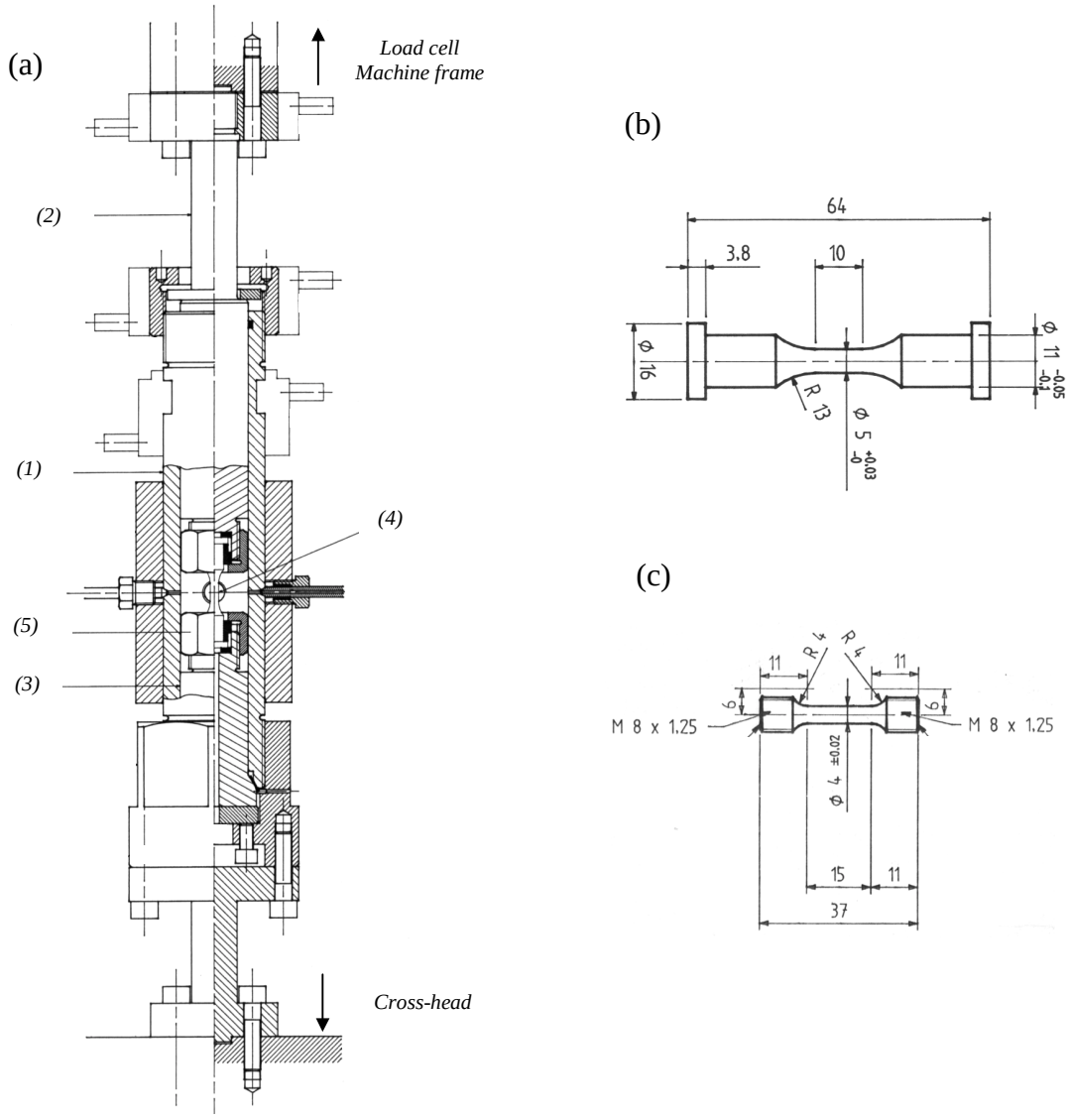

FIGURE 2 – Schematic representations of (a) the autoclave used for CERT testing in aerated supercritical water, (b) the specimens used for CERT testing in aerated supercritical water and (c) the specimens used for CERT testing in air and under vacuum.

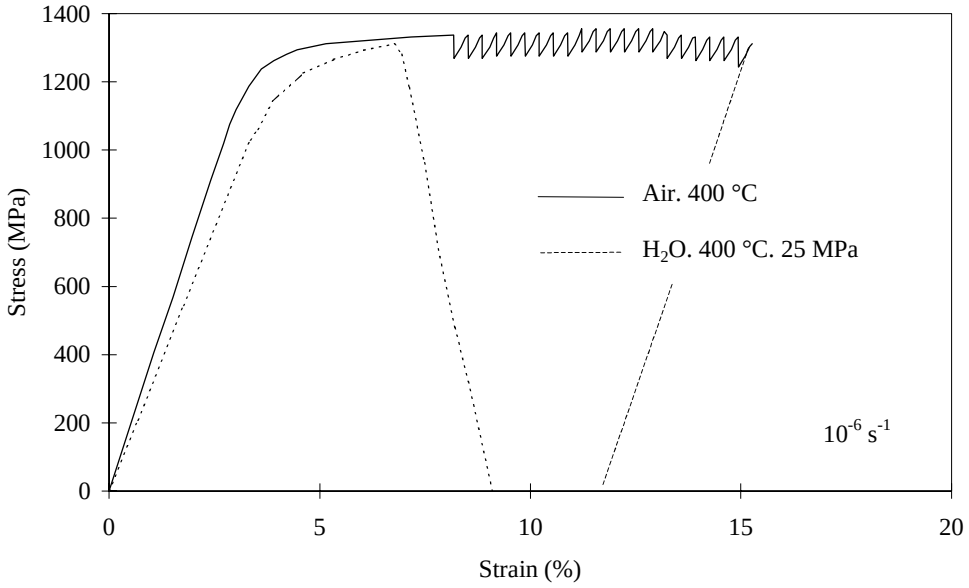

FIGURE 3 – Stress-strain curves from CERT tests conducted at 10^{-6} s^{-1} on alloy 718 specimens in aerated supercritical water at 400°C and 25 MPa, and in air at 400°C.

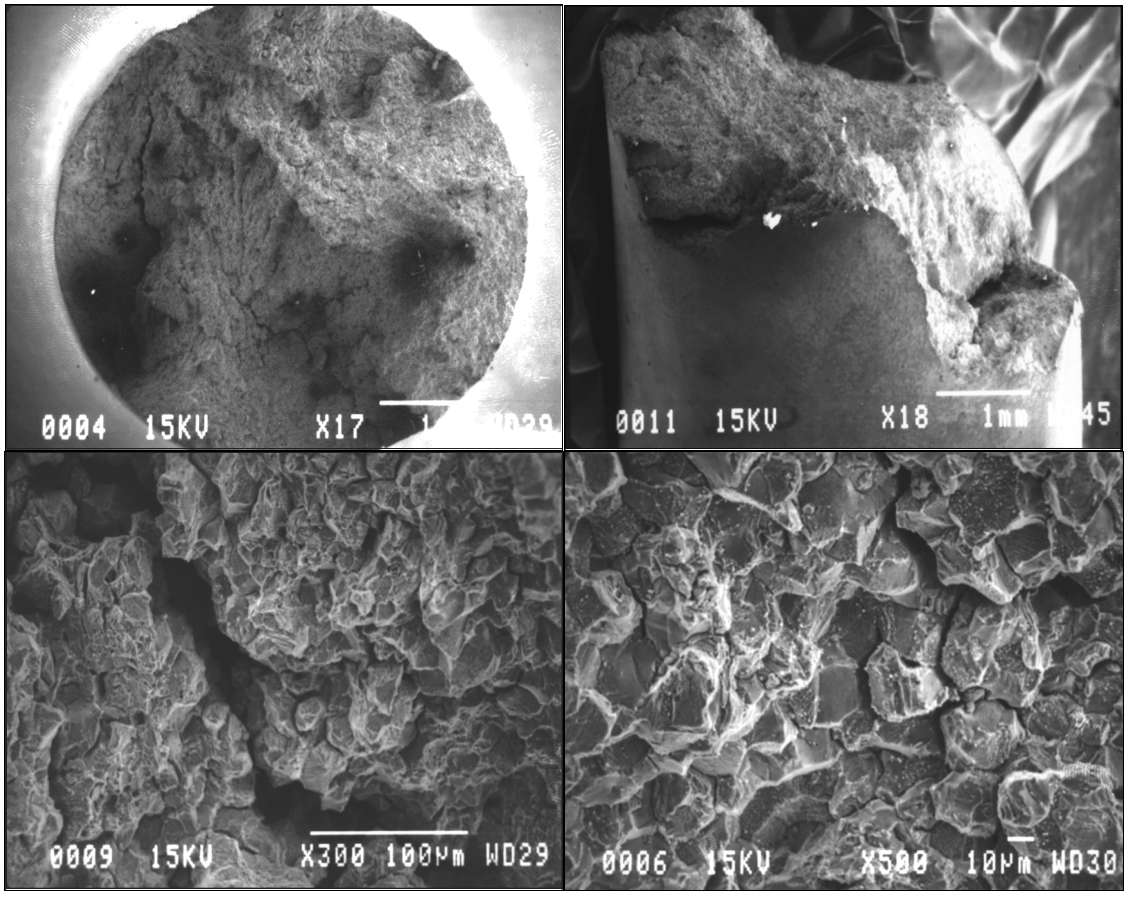

FIGURE 4 – Fracture surface of the alloy 718 specimen deformed at 10^{-6} s^{-1} in aerated supercritical water at 400°C and 25 MPa.

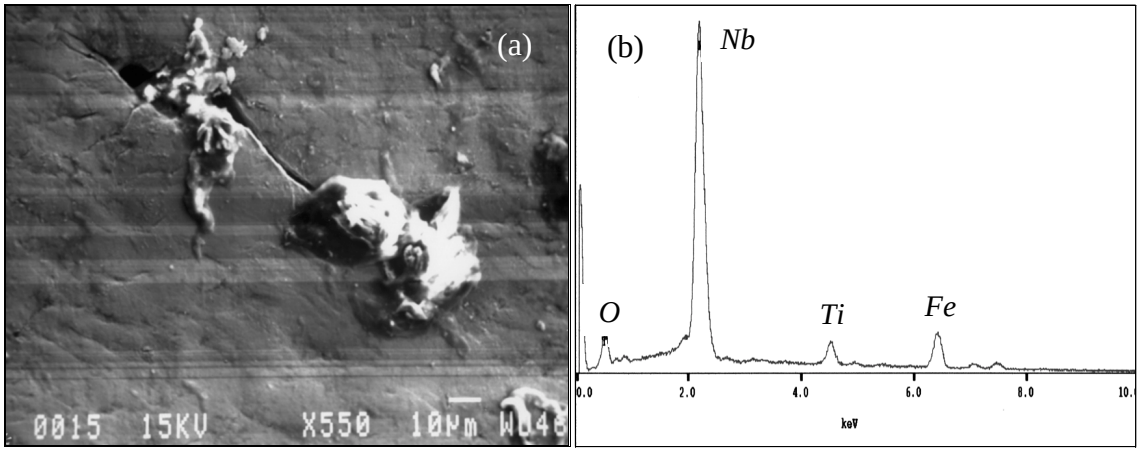

FIGURE 5 – (a) SEM micrograph of the surface of the alloy 718 specimen strained at 10^{-6} s^{-1} in aerated supercritical water and (b) EDX spectrum of the oxidised particle displayed in (a).

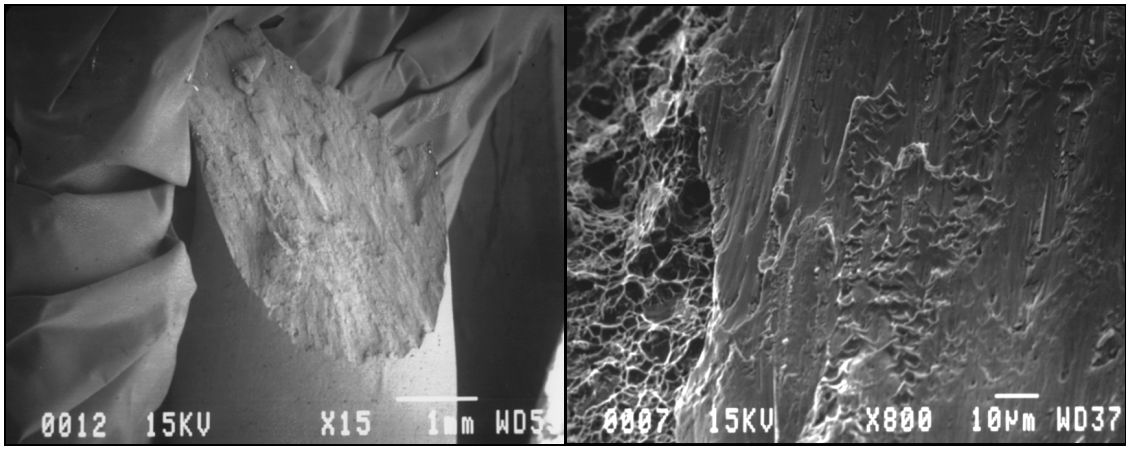

FIGURE 6 – Fracture surface of the alloy 718 specimen deformed at 10^{-6} s^{-1} in air at 400°C.

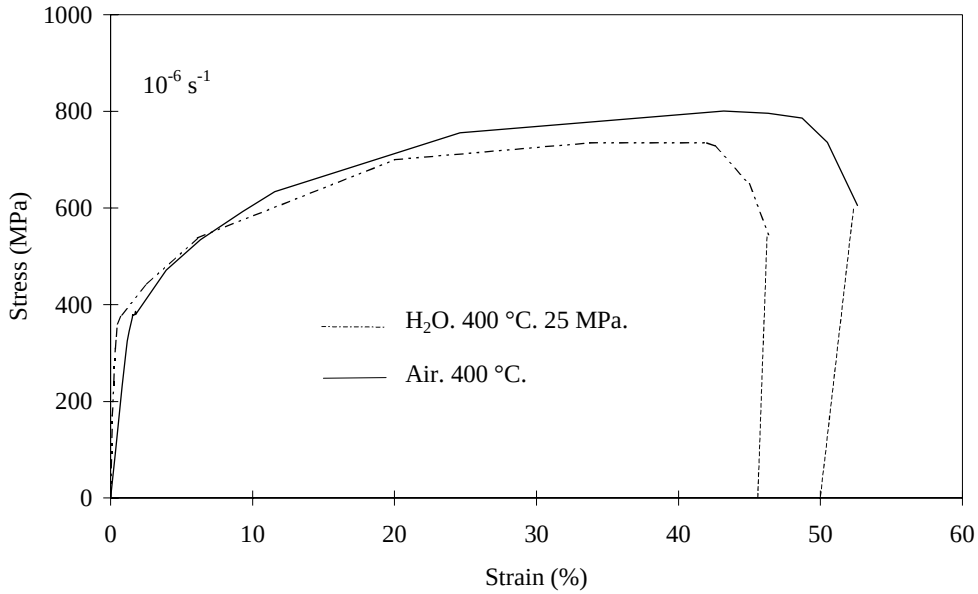

FIGURE 7 – Stress-strain curves from CERT tests conducted at 10^{-6} s^{-1} on alloy 690 specimens in aerated supercritical water at 400°C and 25 MPa, and in air at 400°C.

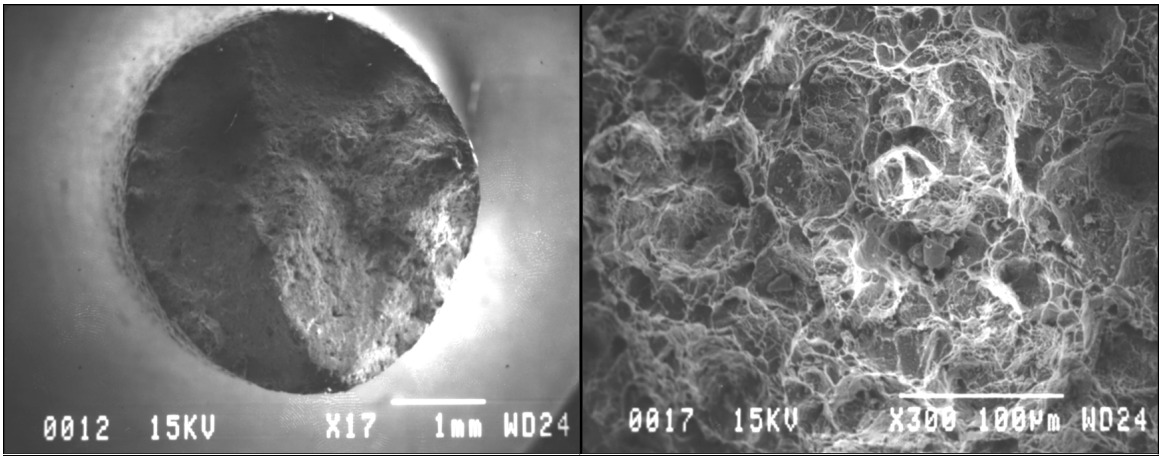

FIGURE 8 – Fracture surface of the alloy 690 specimen deformed at 10^{-6} s^{-1} in supercritical water.

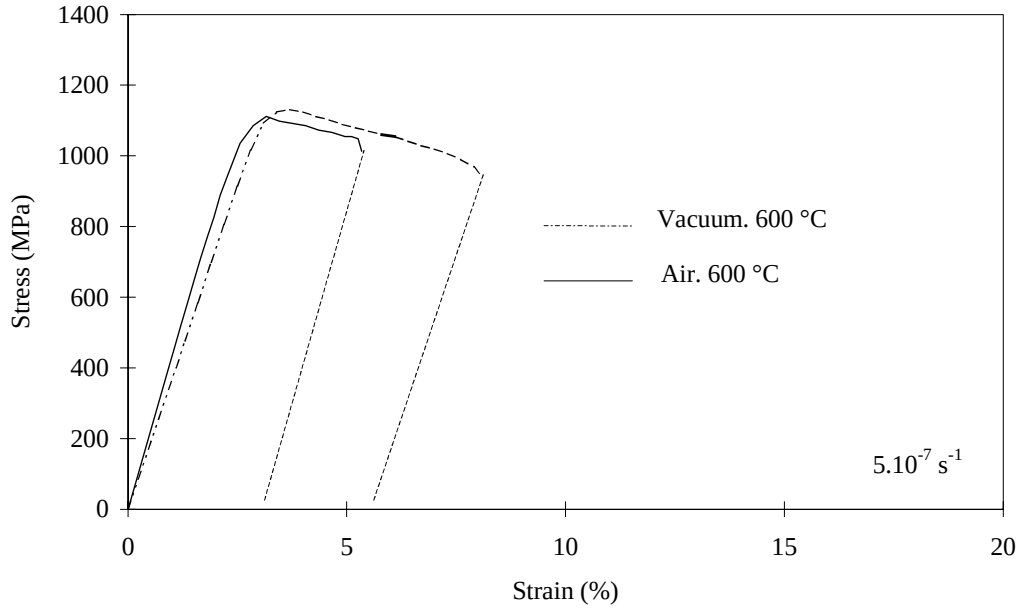

FIGURE 9 – Stress-strain curves from CERT tests conducted at 5×10^{-7} s^{-1} on alloy 718 specimens in air and under vacuum at 600°C.

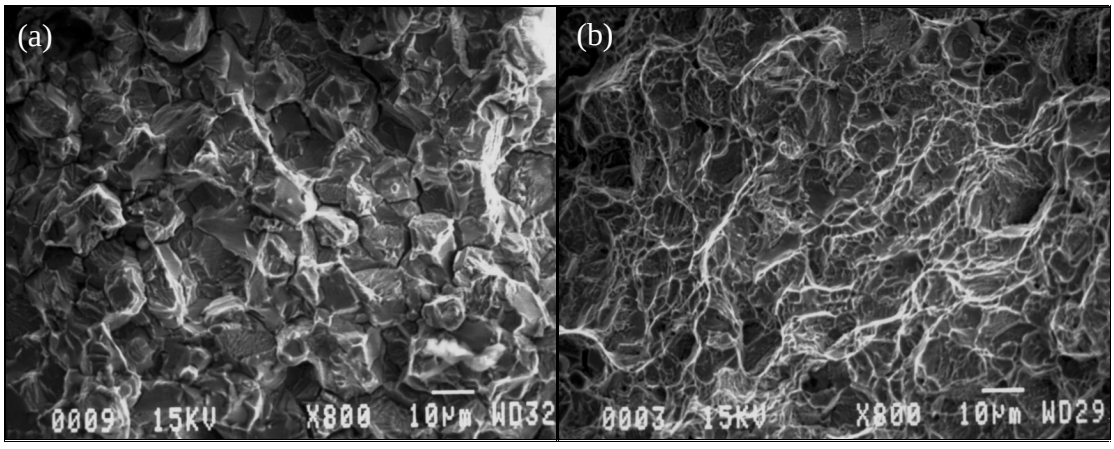

FIGURE 10 – Fracture surface of the alloy 718 specimens deformed at 5×10^{-7} s^{-1} and 600°C (a) in air and (b) under vacuum.

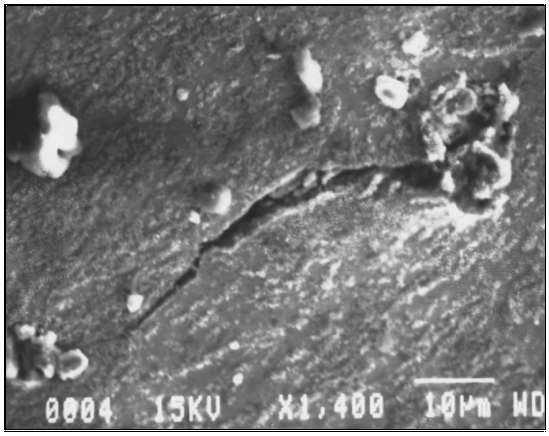

FIGURE 11 – SEM micrograph of the surface of the alloy 718 specimen strained at 5×10^{-7} s^{-1} in air at 600°C.

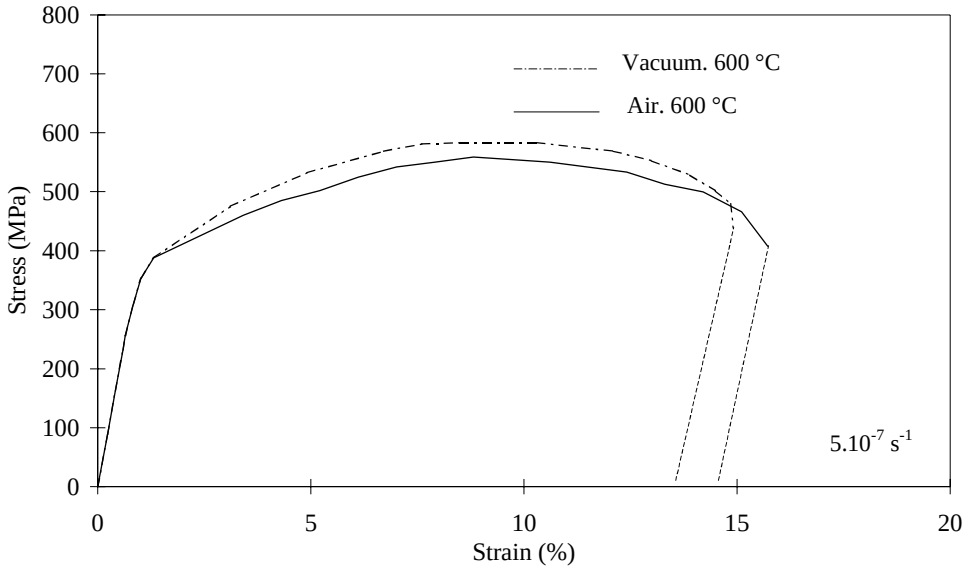

FIGURE 12 – Stress-strain curves from CERT tests conducted at 5×10^{-7} s^{-1} on alloy 690 specimens in air and under vacuum at 600°C.

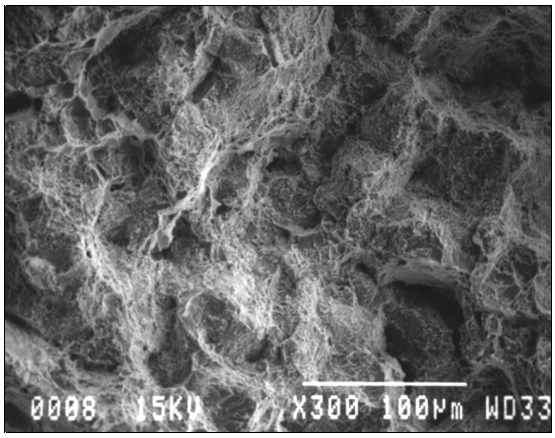

FIGURE 13 – Fracture surface of the alloy 690 specimens deformed at 5×10^{-7} s^{-1} in air at 600°C.